

**Low-Adiabat Implosions:** The adiabat  $\alpha$  of a fluid is defined as the fluid pressure divided by the pressure of the fluid if it were Fermi degenerate. A fluid that is Fermi degenerate requires the least energy to be adiabatically compressed to high densities. The compression of ICF shells to ignition conditions with reasonable drive energy requires that these targets be compressed on as low an adiabat as possible. Shell compression is an unstable process. The Rayleigh–Taylor instability (RTI) occurs when the light fluid of the corona “pushes on” the heavy fluid of the shell and when the shell is decelerated by the hot, low-density gas filling the shell. The RTI growth is reduced by material ablation from the shell—the faster the ablation the lower the RTI growth. Shells with a high adiabat ablate material at higher velocities than shells on a low adiabat. A low shell adiabat is required to compress the target while a high adiabat improves target stability. A series of low-adiabat implosions have been performed with the OMEGA laser to optimize the shell adiabat and to understand the transition from 1-D energetics and compression to multidimensional stability and target performance.

Targets with 27- $\mu\text{m}$ -thick shells were imploded with  $\alpha$ 's of 2, 3, and 5. Figures 1 and 2 show the fuel-areal-density ( $\rho R$ ) measurement for 15- and 3-atm  $\text{D}_2$ -filled targets, respectively. Figure 3 shows the neutron yield for the 15-atm  $\text{D}_2$ -filled targets. Both targets show maximum  $\rho R$  when imploded on an adiabat of  $\alpha \sim 3$ . All data points are averaged over the number of similar shots. The 15-atm  $\alpha \sim 3$  targets have a measured  $\rho R$  of  $120 \pm 4 \text{ mg/cm}^2$  and the 3-atm targets have a measured  $\rho R$  of  $140 \pm 7 \text{ mg/cm}^2$ . The  $\rho R$  in these experiments was inferred by measuring the energy loss of secondary protons (initial average energy  $\sim 15 \text{ MeV}$ ) using wedged range filters.<sup>1</sup> The high  $\rho R$ 's of the 3-atm-filled targets are at the upper measurement limit of the current set of wedged range filters. In both figures the experimental data are plotted as red diamonds, the 1-D shell  $\rho R$  as a solid blue diamond, and the 1-D total  $\rho R$  as an open blue diamond. Two-dimensional DRACO simulations were completed for the 15-atm-filled targets and are plotted in Fig. 1 as open circles with a dashed line. The 2-D simulations show the same trend as the experimental data. The measured  $\rho R$  peaks at an adiabat of  $\sim 3$  in general agreement with 2-D DRACO simulations. The same trend is seen for the neutron yields as plotted in Fig. 3. Both the experimental yield and the yield from 2-D simulations are the largest for an  $\alpha \sim 3$  implosion. These experiments confirm that target stability and compression can be optimized by controlling the shell adiabat. In the future, a similar approach will be applied to targets that can be scaled to ignition conditions.

**OMEGA Operations Summary:** A total of 119 OMEGA target shots were taken in October for LLE (64 shots), LLNL (44 shots), and an NLUF campaign led by the University of California at Berkeley (11 shots). The LLE shots were carried out for the following campaigns: astrojet (10 shots), integrated spherical experiments (31 shots), cryogenic targets (3 shots), LLE National Ignition Campaign (NIC) (18 shots), and long-scale-length plasma interaction (2 shots). The LLNL series included 38 shots for NIC experiments and 6 shots for high-energy-density (HED) physics experiments.

1. F. H. Séguin *et al.*, Phys. Plasmas **9**, 2725 (2002).

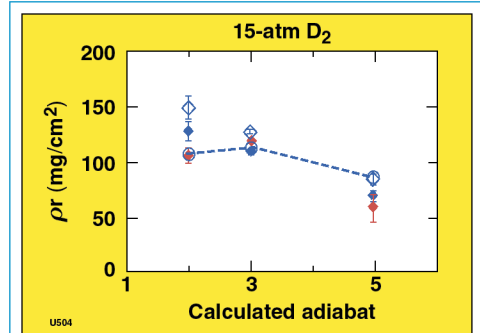


Figure 1.  $\rho R$  as a function of the calculated shell adiabat for 15-atm,  $\text{D}_2$ -filled, 27- $\mu\text{m}$ -thick CH shells. The experimental data are plotted as red diamonds, 1-D LILAC simulation total  $\rho R$  as blue diamonds and 1-D shell  $\rho R$  as open blue diamonds. Two-dimensional DRACO simulations are plotted as open blue circles with a dashed line.

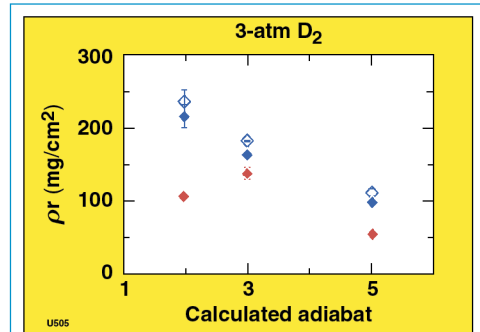


Figure 2.  $\rho R$  as a function of the calculated shell adiabat for 3-atm,  $\text{D}_2$ -filled, 27- $\mu\text{m}$ -thick CH shells. The experimental data are plotted as red diamonds, 1-D LILAC simulation total  $\rho R$  as blue diamonds, and 1-D shell  $\rho R$  as open blue diamonds.

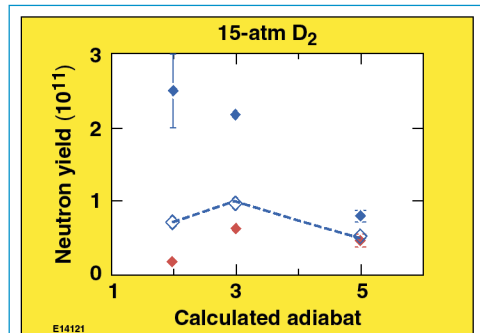


Figure 3. Neutron yield as a function of the calculated shell adiabat for 15-atm,  $\text{D}_2$ -filled, 27- $\mu\text{m}$ -thick CH shells. The experimental data are plotted as red diamonds, 1-D LILAC simulation yield as solid blue diamonds, and 2-D DRACO yields as open blue diamonds.